DRD No. SE-7
DRL No. 58

LOW COST SOLAR ARRAY PROJECT
Large Area Silicon Sheet Task

Dist. Category UC-63
DOE /JPL 954654-79/3

SILICON WEB PROCESS DEVELOPMENT

QUARTERLY REPORT

April 20, 1979-June 30, 1979

C. S. Duncan, R. G. Seidensticker, R. H. Hopkins,
J. P. McHugh, F. E. Hill, M. E. Heimlich, J. M. Driggers
Westinghouse Research & Development Center
Pittsburgh, Pennsylvania 15235

Contract No. ~~NAS~~ JPL 954654

"The JPL Low-Cost Silicon Solar Array Project is sponsored by the U. S. Department of Energy and forms part of the Solar Photovoltaic Conversion Program to initiate a major effort toward the development of low-cost solar arrays. This work was performed for the Jet Propulsion Laboratory, California Institute of Technology by agreement between NASA and DOE."

Westinghouse R&D Center
1310 Beulah Road
Pittsburgh, Pennsylvania 15235

LOW COST SOLAR ARRAY PROJECT
Large Area Silicon Sheet Task

SILICON WEB PROCESS DEVELOPMENT

QUARTERLY REPORT

April 20, 1979-June 30, 1979

C. S. Duncan, R. G. Seidensticker, R. H. Hopkins,
J. P. McHugh, F. E. Hill, M. E. Heimlich, J. M. Driggers
Westinghouse Research & Development Center
Pittsburgh, Pennsylvania 15235

Contract No. ~~NAS~~ JPL 954654

"The JPL Low-Cost Silicon Solar Array Project is sponsored by the U. S. Department of Energy and forms part of the Solar Photovoltaic Conversion Program to initiate a major effort toward the development of low-cost solar arrays. This work was performed for the Jet Propulsion Laboratory, California Institute of Technology by agreement between NASA and DOE."

Westinghouse R&D Center
1310 Beulah Road
Pittsburgh, Pennsylvania 15235

TECHNICAL CONTENT STATEMENT

"This report was prepared as an account of work sponsored by the United States Government. Neither the United States nor the United States Department of Energy, nor any of their employes, nor any of their contractors, subcontractors, or their employees, makes any warranty, express or implied, or assumes any legal liability of responsibility for the accuracy, completeness or usefulness of any information, apparatus, product or process disclosed, or represents that its use would not infringe privately owned rights."

TABLE OF CONTENTS

LIST OF ILLUSTRATIONS

LIST OF TABLES

1. SUMMARY

Silicon dendritic web is a ribbon form of silicon produced from the melt without die shaping, and capable of fabrication into solar cells with greater than 15% AM1 conversion efficiency. This is the first quarterly report on Phase III of DOE/JPL-sponsored effort to develop silicon web process technology compatible with the national goals for low cost photovoltaic output power.

During the approximately one and a half month period covered by the report, significant improvements have been made both in the width of the web ribbons grown, and in the techniques to replenish the liquid silicon as it is transformed to web. For example, we have by means of improved thermal shielding reduced stress sufficiently that web crystals nearly 4.5cm wide have been grown.

We previously showed that melt replenishment is required to sustain stable, high output rate web growth for protracted periods. We have continued the development of two subsystems: a silicon feeder and a melt level sensor, necessary to achieve an operational melt replenishment system. Utilizing a newly-designed gas flow management technique, coupled with improved thermal shielding, we have doubled to two hours the period for which web is grown with simultaneous silicon feeding. To sense and control the melt level as silicon is replenished we have identified, and successfully bench tested, a laser reflection method. A conceptual design of the level sensor has been made and system components ordered.

A new web growth furnace built at Westinghouse expense has been completed and is now operational. This unit will be dedicated to the JPL program, primarily for the development of techniques to enhance web output rate.

Finally we have measured the effective segregation coefficient of boron in silicon during web growth, a parameter necessary to precisely dope (control resistivity) web solar cells. We find $k_{eff} = 0.7$, a value somewhat lower than usually quoted for Czochralski pulling (0.8).

2. INTRODUCTION

Silicon dendritic web is a ribbon form of silicon which grows directly from the melt without dies and can produce solar cells with AM1 conversion efficiency over 15%. The primary objective of this program is to develop the technology to produce silicon web at a cost compatible with the national goal of 50 cents per peak watt (70 cents per watt in 1980$) of photovoltaic output power.

This is the first quarterly report of the Phase III effort under JPL Contract 954654, Silicon Web Process Development, and covers the period (April 20, 1979 to June 30, 1979) since the publication of the Annual Report[1] of Phase II. This report is thus necessarily brief, covering the technical highlights of recent activity.

Readers are referred to Reference 1 for a detailed description of the major technical results underlying the development of silicon web for low cost solar cells. Briefly, we showed there that most of the technical requirements to meet the 1986 cost goals have now been demonstrated. However, to sustain the necessary area output rates, and to grow web for periods long enough to attain economic viability, the development of an operational melt replenishment system and closed-loop growth system controls were identified as necessary. These two developments thus form major objectives for the Phase III effort.

Besides the development of replenishment and control techniques, the Phase III technical effort also calls for the systematic evaluation of advanced thermal trimming techniques to increase web width and speed still further, for coupling of output rate and replenishment technologies, design of a semi-automated experimental web growth machine, of detailed characterization of web material produced during the experimental program, and for an update of the economic analysis to reflect new technical and cost information generated during the program.

During the period since the Annual Report effort has proceeded to improve the procedures for feeding silicon while simultaneously growing web and also to design a liquid level sensor, a precursor for closed loop control of the melt replenishment. Also, improved thermal shielding above the melt has produced the widest web to date, nearly 45 mm across. We have also brought on line at Westinghouse expense new web growth facilities, one of which will be dedicated to use on the Phase III program. Finally, we have measured the segregation coefficient for boron during web growth, a parameter of some importance for controlling material resistivity during experimental and production operations. The highlights of the work are described in subsequent report sections; the details of the experimental runs are collected in the Appendix, a procedure we have followed in past reports.

3. TECHNICAL PROGRESS

3.1 Background

In reality, there are three components that must be considered to improve web output rate: crystal width, growth velocity, and maintenance of melt height at the optimum level. (The various factors which impact output and the parameters which can be manipulated have been discussed in detail in previous reports and will not be repeated here; See, for example, Reference 1). Although the three components are not completely decoupled, particularly in terms of constraints that one may impose on another, considerable progress can be made if the technologies are developed in parallel efforts, and combined then as individual advances in technology are achieved.

During this reporting period, the major efforts have been devoted to width improvement and to melt replenishment development. A new furnace facility which will shortly become operational (see Section 3A) will be utilized for growth velocity studies, so that development activities for all three rate components can be carried on simultaneously. It should be noted that the internal configurations (susceptor, lids, shields, etc.) are completely interchangeable among the three furnace facilities, so that transfer of technology from one furnace to another is a straight forward operation. We have shown earlier that the same configuration gives the identical performance independent of the furnace in which it is employed.[1]

3.2 Width Enhancement

The J-furnace was dedicated to width improvement during this reporting period. Although area throughput was a secondary objective, rates greater than 20 cm^2/min were achieved several times (See Appendix 9.1). This was possible because the base line lid being used in the

width studies is a fairly "fast" design, the logic being that in this way improved width may be more readily extended to improve area output rates. Furthermore, advances in speed and width technology must lead to configurational features which are compatible if optimum area output rates are to be realized.

Some recent results in terms, both output rate and widths, are compiled in Table 1. Where growth velocities are not given, the values generally varied during the growth period, so as to maintain thickness as the melt level dropped. Note that the wider the crystal, the faster the melt is depleted.

The problem is not insignificant. For example, two extreme results of melt depletion during crystal growth are illustrated in Figure 1. In these cases, so much silicon had been pulled from the melt that the melt level became so low that it was unstable against surface tension forces; the melt pulled away from the periphery of the crucible. This, of course, terminates growth.

As has been discussed previously, the limiting factor in crystal width has been stress-induced deformation, which at some point causes a degradation in crystal quality.[1] Thermal modeling results indicated that the temperature distribution in the web in the vertical direction has a substantial impact on the amount of stress generated in the growing web. Specifically the stress is greatly reduced if the portion of the web a short distance above the lid "sees" a cool environment. Experiments with a cold aftertrimmer whose function was to shield the crystal from the hot growth lid did indeed result in low stress web crystals. However, the aftertrimmer, at least as then configured, produced gas convective effects so that the expected potential in terms of width enhancement could not be realized.[1]

Another method which accomplishes some of the basic function of the cold trimmer is to shape the vertical temperature distribution in the web by modifications in the top shield configuration, including the number, shape, and relative positioning of the shields. Some of the variations recently tested are illustrated in Figure 2. For reference,

TABLE 1

SOME RECENT THROUGHPUT RESULTS AND WIDTH RESULTS

Run No.	Throughput rate cm^2/min	Width mm	Growth velocity cm/min
J-163	21.7	32.5	6.75
J-164	20.0	34.9	5.74
RE-151	-	43.1	-
RE-156	19.6	39.1	5.0
J-165	-	40.5	-
J-173	22.0	32.8	6.7
J-180	-	40.1	-
J-181	-	42.1	-
J-182	-	44.3	-

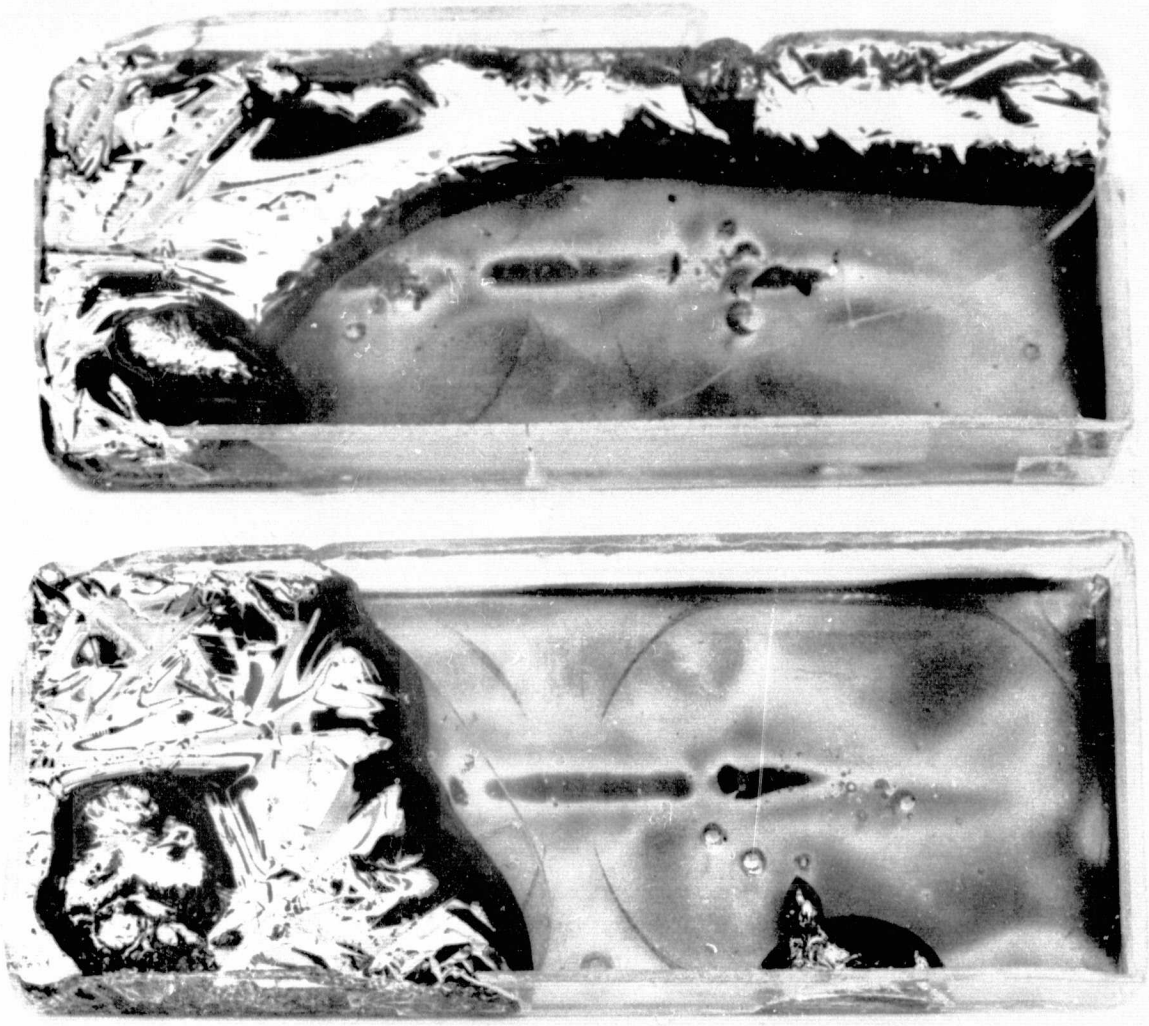

Figure 1 Extreme Effects of Melt Depletion; The Silicon Melt Pulls Away from the Crucible Due to Surface Tension Forces.

Figure 2A shows a cross section of the base line lid and shield configuration used in earlier experiments[1,2]. The top shielding consists of a thin molybdenum shield which is bent to cover the top edge of the beveled lid slot below it. A 1.5 mm thick shield is placed over both lid and intermediate shield. With this arrangement, argon flow tubes parallel to the slot were needed to prevent silicon monoxide from collecting on the lip of the bent shield. This arrangement consistently produced 3.5 to 3.6 cm wide web.

The first variation to this configuration which we tested was simply the addition of a second 1.5 mm thick shield with the same slot shape as the one below, figure 2B. This arrangement immediately yielded increased web width to 4.0-4.2cm in both the J and RE furnaces. An additional benefit gained from this configuration is that the formed or bent shield remained oxide-free without the use of the argon flow tubes, thus simplifying the setup.

An obvious extension to this approach was to add a third thick top shield as in Figure 2C. However, this configuration was unsuccessful; free-floating silicon"ice" repeatly formed on the melt. We suspect that the melt at the crucible wall was not quite hot enough to prevent nucleation due to the flattened thermal profile in the liquid.

Another shield variation, shown in Figure 2D, comprised a thin (0.5mm) shield laid atop the second thick shield. The widest web crystals so far produced, 4.43cm, have been grown with this setup.

More dramatic than overall width increases has been the increase in width of high quality web crystal before the occurrence of stress-induced deformation or degradation in crystal quality. A gain of 1 cm or more as compared to earlier results has been realized through shield modifications.

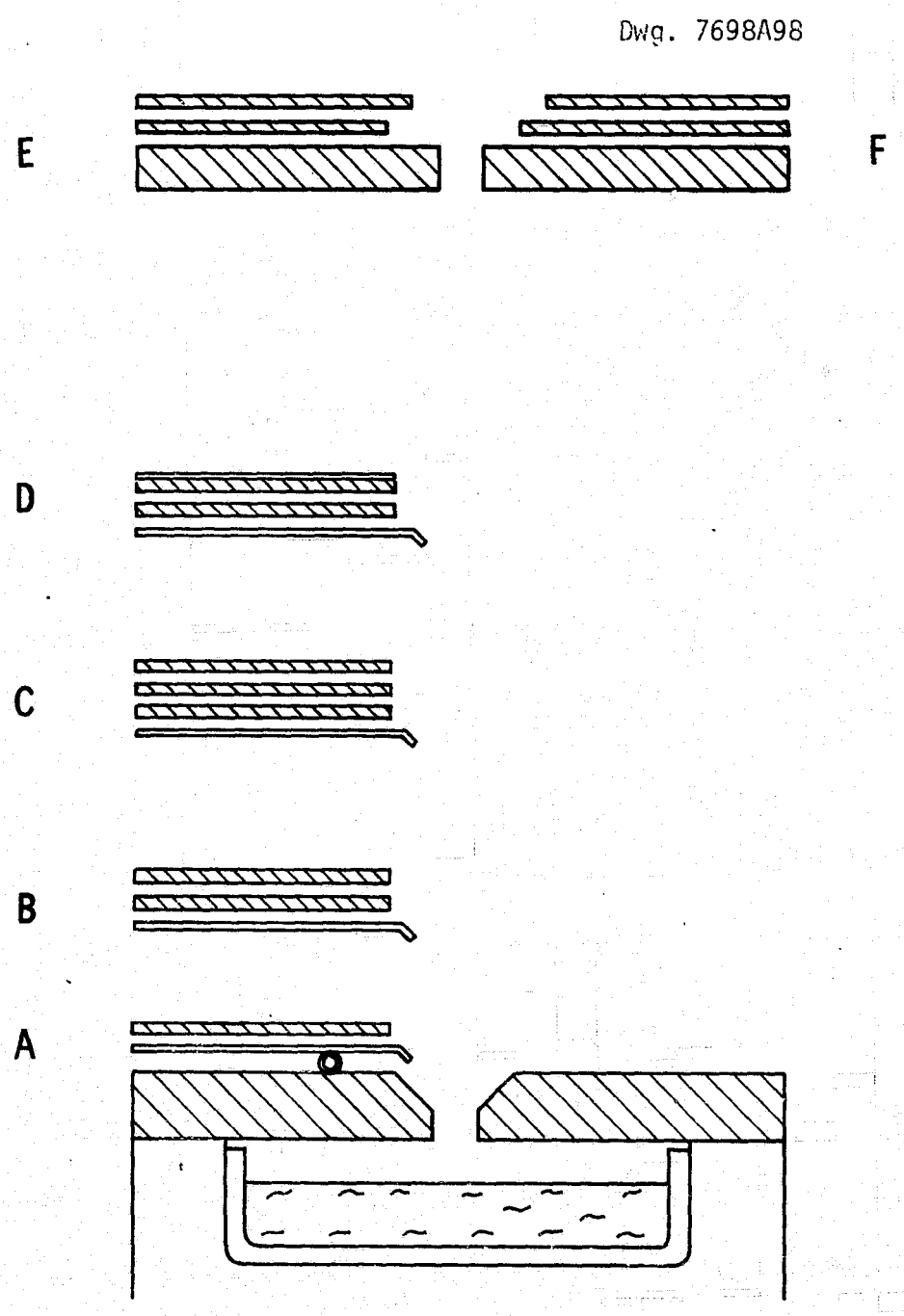

Figure 2 Lid/Shield Configurations to Control the Vertical Temperature Profile in Web Crystals.

One further example of the effects of top shield configuration on growth behavior can be noted with respect to the disparate performances of configurations E and F, Figure 2. The difference between the two arrangements is that the two shields were interchanged; the shield with the larger set back is above in F and below in E. Configuration E, (RE-1 Type shield arrangement) provides excellent growth stability, whereas with configuration F the dendrites are very non-uniform in thickness and spontaneous pullouts or extra dendrites occur with excessive frequency.

The approach of modifying vertical temperature distributions via top shield configurations offers a method of fine tuning the thermal profiles within the web over the region near the lid. We expect to pursue this approach further. At the same time, an effort will be made to redesign the cold aftertrimmer to eliminate the negative effect on growth behavior. This will expand our capabilities for temperature distribution control.

3.3 Melt Replenishment Development

3.3.1 Silicon Feeding Technique

Previously we established the utility of controlled gas flow (to minimize oxide deposition during feeding) and a mechanized pellet feeder for simultaneously growing web while replenishing the melt with silicon.[1,2] The experiments were carried out on the W furnace whose small, round susceptor is thermally unacceptable for prolonged, high output rate operation. During this quarter we carried out experiments to transfer this technology to the elongated susceptor in the RE furnace which is compatible with our technical objectives. The details of the experiments appear in Appendix 9.1; the salient results are recorded below.

In Figure 3 the mechanized feeder is shown remounted in position on the RE furnace. The unit permits silicon pellets to be metered through a quartz tube to the melt at rates between 1 and 10 pellets per minute. This range is sufficient to replenish the silicon

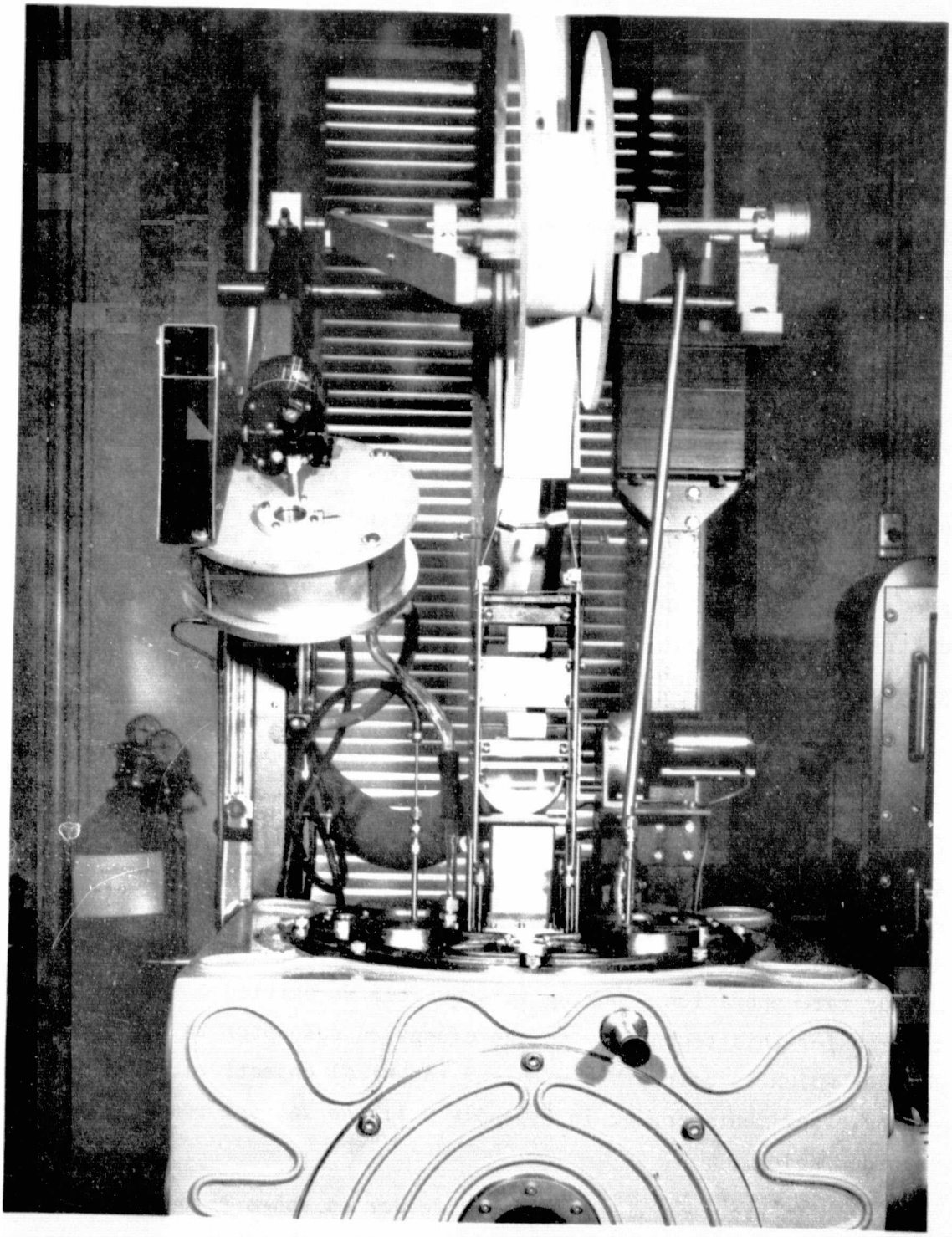

Figure 3 Mechanized Pellet Feeder Mounted for Operation on the RE Furnace.

consumed during web growth at the output rates we expect to achieve during the program. Operation of the feeder is described in Reference 1.

Initial replenishment runs were to test suitable configurations of the aspirator system used to control oxide deposition during feeding in the RE furnace. We found that aspirators like those used in the W-furnace (Figure 31, reference 1) became blocked with oxide within an hour after the silicon was molten. This difficulty was circumvented by making the aspirator channel an integral part of the lid as suggested in Figures 4 and 5. A slot was milled in the lid into which the jet is inserted. The arrows in Figure 4 indicate how the gas and oxide are swept away from the direction of the growing crystal and exhausted from the susceptor end. The cutaway view in Figure 5 indicates the relative positions of the various components. This system remains clean and unblocked during operation.

The presence of the feed hole and the aspirator on the same end of the susceptor depresses the temperature of the feed end. In order to add pellets without causing the melt to freeze, additional shielding was required. As experience with this shielding and the adjustment of the coil position was gained, the pellet feed rate and the length of successful growth periods both increased (viz, Appendix).

The longest feeding period obtained so far was about two hours or nearly twice that previously achieved.[1] The crystal growth was ended when an increase in feed rate caused ice. In another run of similar duration, growth ended after the web began to deform, a problem not related to feeding. Because the consistency of the feeding experiments and their duration was improving, it became evident that further development of feeding would require growth lids for which longer growth periods could be achieved without web deformation. To do this, a parallel development of feed lids designed to accommodate wider and longer web crystals was undertaken.

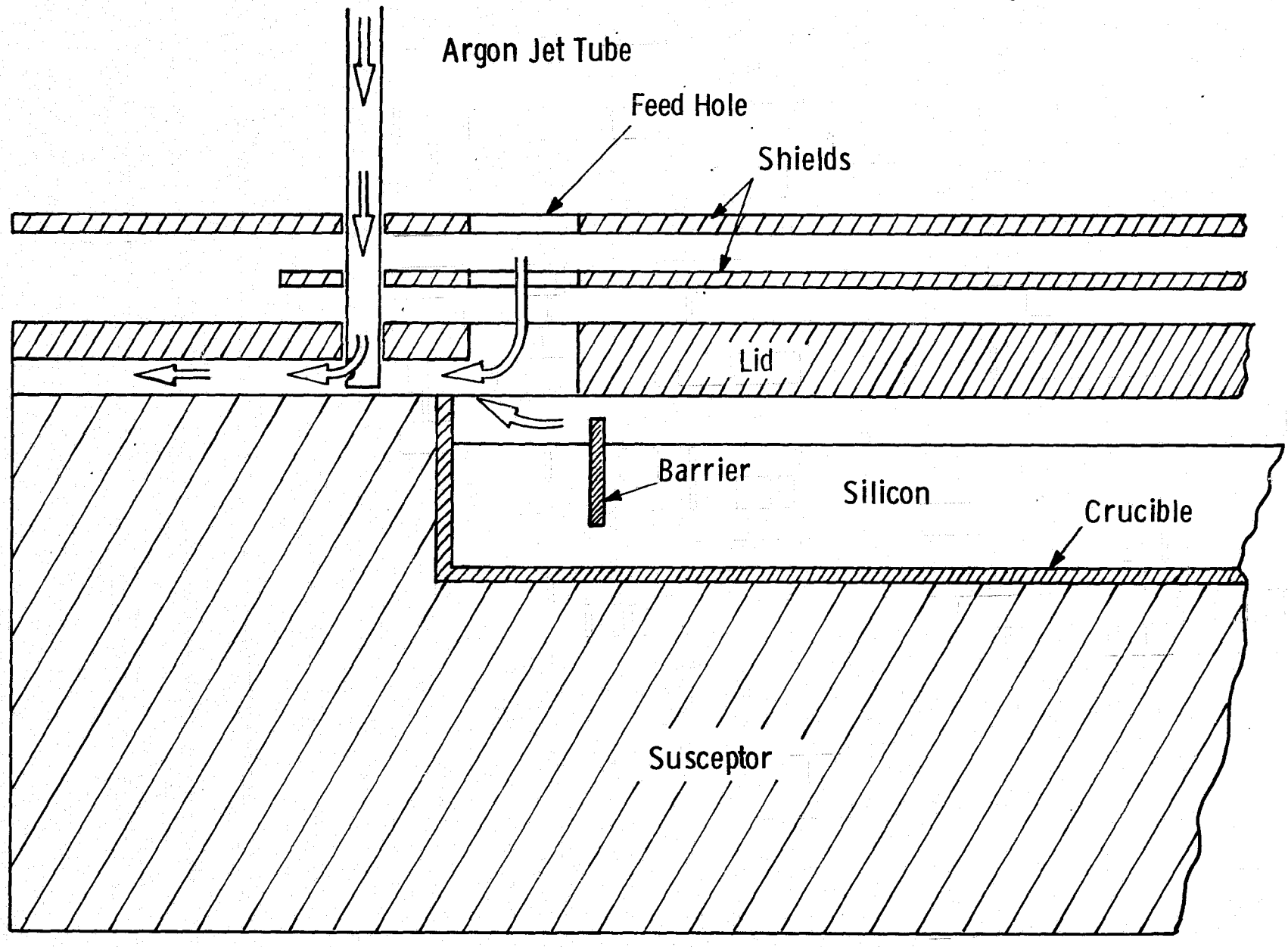

Figure 4 Milled Aspirator, Used with Elongated Susceptor in RE Furnace to Control Oxide. Arrows Indicate Argon Flow Path.

Dwg. 7699A80

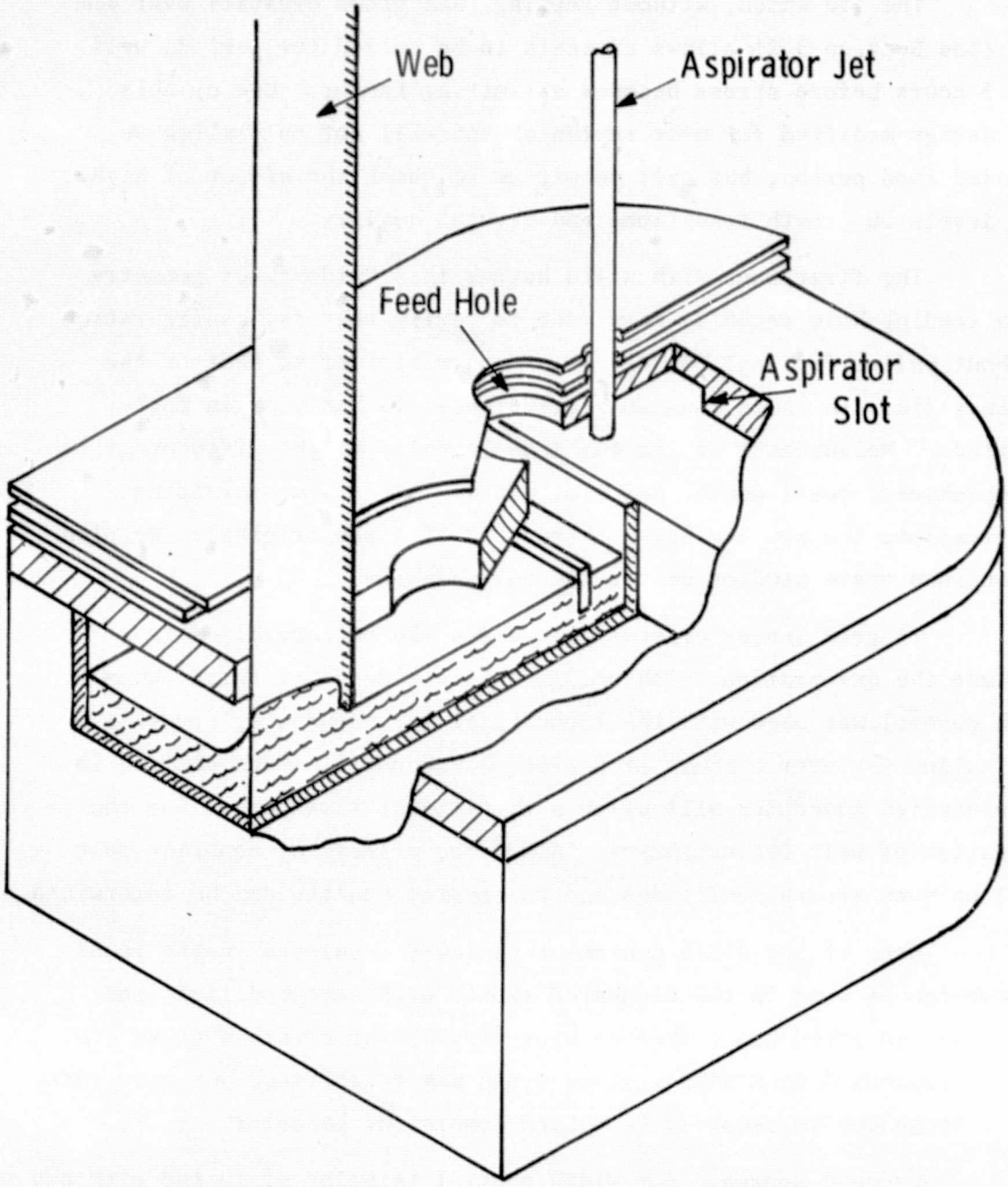

Figure 5 Partial View of Elongated Susceptor with Feed Hole and Aspirator in Place.

The lid which, without feeding, has grown crystals over 4cm wide (see Section 3.2) allows crystals to be pulled for periods well over 3 hours before stress becomes a limiting factor. Use of this slot design modified for melt replenishment will not only allow an extended feed period, but will permit us to check the effect of higher melt levels on growth conditions and crystal quality.

The first runs with a lid having this "wide" slot geometry and a feeding hole recently were made to verify that the configuration (without pellet feeding) behaved in a manner similar to that of the original lid. In these runs some differences in behavior in fact occurred. Measurement of the two lids revealed slight differences in lid thickness, bevel depth, and slot width. After some shielding modifications the new lid began to respond like the original. We plan to continue these studies during the next quarter.

To grow longer crystals, web width may be controlled to preclude the deformation which occurs in the widest crystals. When width control was used with the round susceptor W-furnace, crystals were pulled for over 6 hours at a time.[1] Successful width control in the elongated susceptor will allow a significant time period for the evaluation of melt replenishment. Also, the effects of constant melt level on both growth conditions and on crystal quality can be determined.

Many of the width control techniques developed in the round furnace can be used in the elongated system with some modifications. The first lid tried had a shorter slot length; the crystals grown did exhibit regions where a steady-state width was established but more work on the technique is required to obtain consistent behavior.

A second approach for width control is being evaluated with the long growth slot lids. In this arrangement, the effective slot length can be adjusted (shortened) as the crystal reaches a target width. Movable molybdenum shields will be used to make the dynamic changes. Experiments in the development of this technique have just begun.

3.3.2 Melt Level Sensing

In order that melt replenishment be fully utilized it is essential that the rate of replenishment be controlled to provide a constant melt level. The key component to such control is a transducer which expresses the melt level position in terms of an electrical signal. The transducer in essence determines the system for melt level sensing. Once the melt level is expressed in terms of a suitable electrical signal, both measurement and control of the melt level are readily attained.

It is our intention initially to use the electrical signal only in a measurement mode in order that the now-existing motor driven polysilicon pellet feeder may be programmed at a rate which will approximate a constant melt level. Closed loop control to provide active melt level control will be added later.

The first step in selecting a method of melt level sensing was to consider the system requirements. The main requirements are largely self-explanitory. The sensor:

- Must be compatible with web growth and the web growth apparatus,
- Must be accurate to within one millimeter or better,
- Must be capable of both measurement and control,
- Must maintain calibration during a growth cycle, and
- Must be of reasonable cost.

A number of candidate methods for melt level sensing were considered, including:

(1) Reflected beam of coherent light (laser) used with various electro-optical position sensors.

(2) Same as (1) except non-coherent light source.

(3) Distance sensing by direct reflection, as with radar or sonar.

(4) Direct observation by light or other transmission through susceptor and crucible.

(5) Weight transducers.

(6) Electrical contact to the melt.

(7) Capacitive (proximity) effect.

Method (1) was selected for demonstration because it appeared to be rather clearly more favorable in a number of ways than the others, although methods (2) through (7) were each workable at least in principle.

The method selected has been demonstrated in a bench test version and was found to satisfy all requirements for melt level sensing. The bench test employed a two milliwatt helium-neon laser as a light source. The light beam was directed at 45° onto a pool of mercury (to simulate molten silicon) from which it was reflected through a concentrating lens onto a commercial solid state position detector. Vertical movement of the mercury level produced a shift in laser beam position readily sensed by the detector.

The laser reflection method for melt level sensing was also verified in another way. The laser was temporarily mounted at a viewing window of a growth furnace and aimed onto a silicon melt such that the reflected beam passed through a second viewing window and out of the furnace. The attenuation of the beam during transit through the furnace was found to be insignificant relative to the requirements for level sensing.

The laser system as it will be applied to a web growth furnace is illustrated schematically in Figure 6. The route of the light beam through the growth chamber is almost identifical to the bench test arrangement. The tubular projections from the windows serve to minimize the accummulation of oxide on the window surfaces. (This is merely a precaution since within wide limits, variations in the intensity of the beam do not affect the calibration of the melt level measurement or the quality of control attainable).

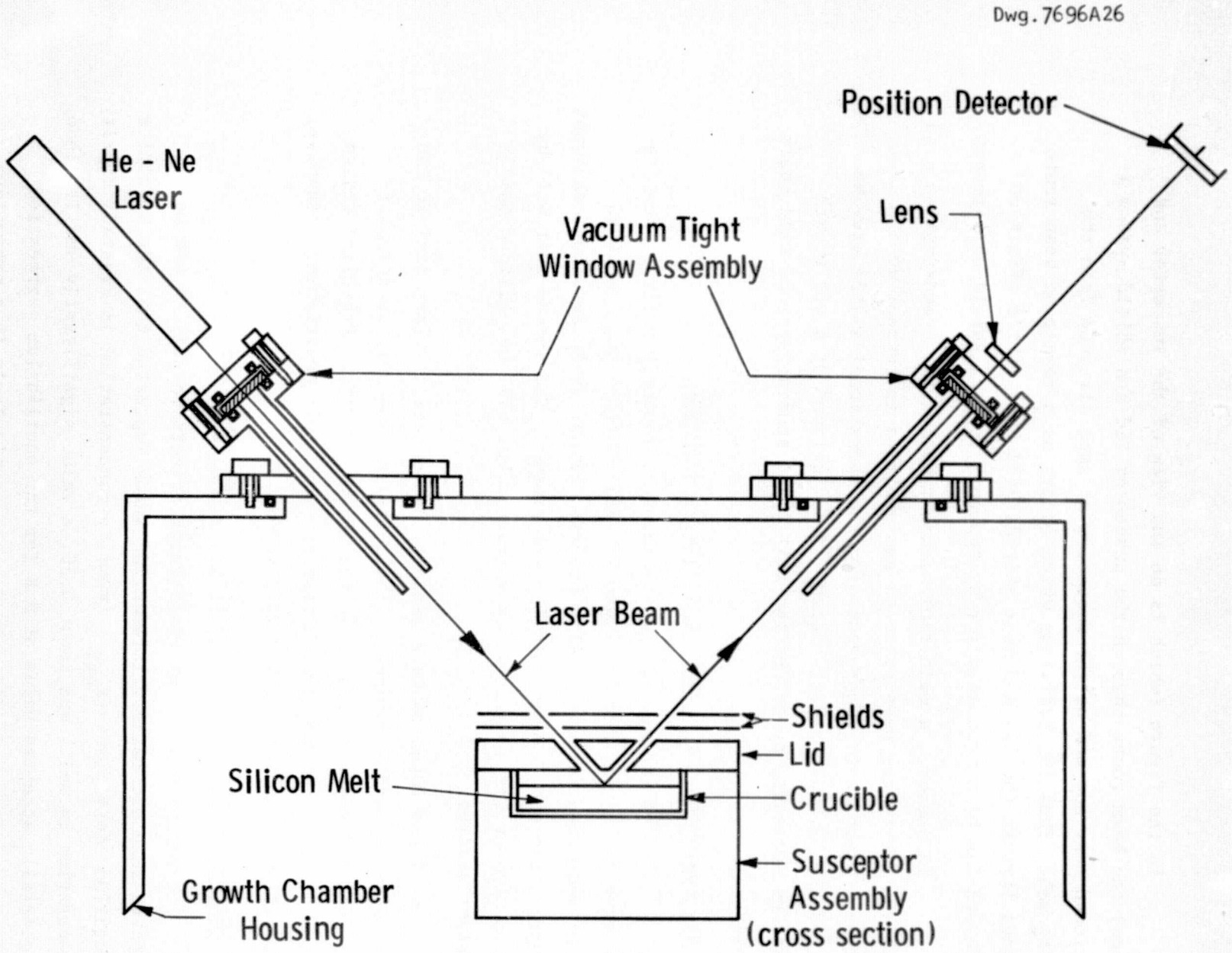

Figure 6 Schematic Depiction of Melt Level Sensor for Web Growth.

In the figure (which is an end view of the susceptor and furnace) the beam route through the susceptor lid and shield system is positioned near one end of the susceptor at some distance from the growing web. Thus,the heat loss which occurs as a result of beam route openings through the lid and heat shields will have little effect on growth,and can be compensated for by appropriate heat shield adjustments.

In summary, a melt replenishment method for demonstration with actual web growth has been selected and verified in concept by a functional bench test. Components for the operational system have been selected and purchase orders placed. Modifications of a web growth furnace as necessary to accept the melt level sensing systems will begin promptly.

3.4 New Equipment for Area Output Rate Development

One of two new web growth furnaces recently built at Westinghouse expense is pictured in Figure 7. This unit is now completed will be dedicated for use on this program, primarily to develop techniques to improve the area output rate for web growth. The second unit will be used to augment the program where warranted but will be utilized mainly for other studies.

These furnaces have capacity and capability identical to the existing JPL RE and J furnaces. Their design, however, is somewhat simplified and lower in cost than the RE and J units. Principal design changes are found in the growth chamber, work coil positioning mechanism, web positioning guides,and vacuum components.

3.5 The Segregation of Boron during Silicon Web Growth

During a study of resistivity effects in silicon web we collected some preliminary information which suggested that the effective segregation coefficient (k_{eff} = impurity concentration in crystal/impurity concentration in melt) was about 0.59, a value significantly smaller than the generally accepted value of 0.8 for the equilibrium segregation coefficient.[1] Since proper melt doping, particularly in a production

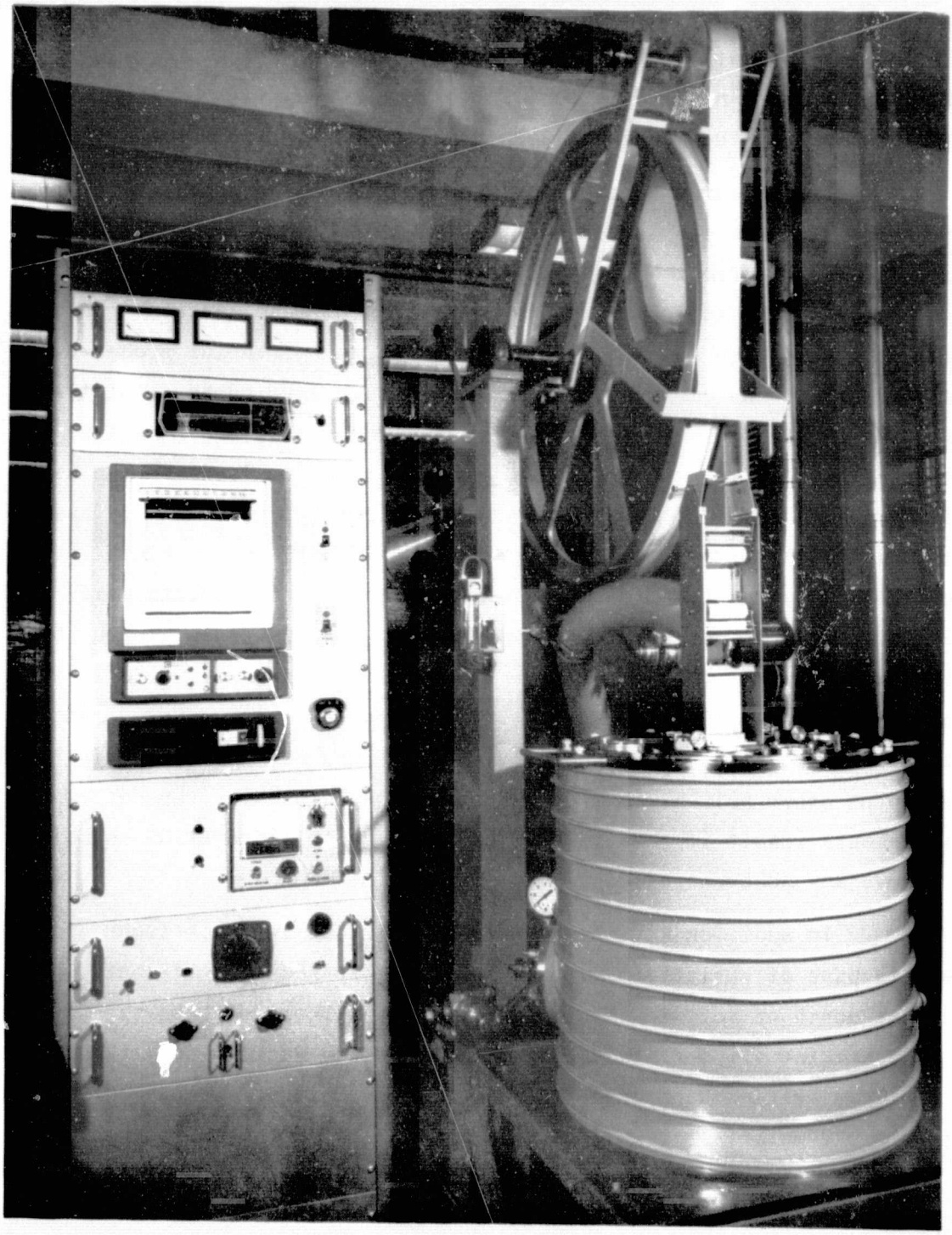

Figure 7 New Westinghouse Web Growth Facility

activity, is necessary to control the resistivity in the subsequently fabricated solar cell, we carried out some further studies to clarify this point. These newer data plus further refinement of the resistivity measurements lead to a somewhat larger value of $k_{eff} = 0.7$.

In the earlier report[1] the geometric factors necessary for the analysis of the raw I-V data were discussed. The use of the appropriate corrections brought more consistency to the resistivity data; however,there was still excessive scatter in some measurements. We then found that a voltage was sometimes present at the potential probes even when no current was present. This potential was very photo sensitive and was probably the result of a metal-insulator--semiconductor type of contact at the voltage probe caused by a spotty oxide layer on the as-grown web surface. The measurement reproducibility and stability has been enhanced by simply covering the probe head with a dark cloth. Further improvement resulted when several measurement currents were employed. In this way,any constant photovoltage was cancelled out by using $\Delta V/\Delta I$ rather than V/I in the calculation: $\rho_B = CtV/I$ (C is the geometric factor and t is the sample thickness). Proper sample preparation also improves the reproducibility of the measurements: swabbing with acetone or other solvent to remove loose oxide helps but even better measurements result if this initial cleaning is followed by HF swabbing to remove any adherent oxide film.

In addition to improved measurement and analysis techniques, the data base of resistivity values has been expanded significantly in the last month or so. We also traced the lot numbers of both the polycrystalline silicon starting material and the Dopesil* pellets used to dope the melt with boron. Data for four different Dopesil lots and for some old material grown from a "master alloy" doped melt are listed in Table 2. All the melts represented by the Dopesil data were prepared from the same lot of polycrystalline silicon.

* Trademark of Dow Corning Corporation.

TABLE 2

MEASURED BORON SEGREGATION COEFFICIENTS FOR SILICON WEB GROWTH

Dopant Lot Number	Nominal Boron Content	Number of Samples	Resistivity Range	Effective Segregation Coefficient
WPD-006	$2x10^{17}$	15	6.5-10.3	.72±.09
WPD-007	$3x10^{17}$	12	1.7-4.6	.67±.07
WPD-023	$2x10^{17}$	7	6.5-9.5	.69±.12
WPD-026	$2x10^{17}$	21	5.9-10.5	.72±.14
"Master Dope"		2	4.3-4.4	.68±.01
		Grand Average		.70±.03

Earlier we felt there was some systematic variation in boron content between Dopesil lots, but this conjecture is not supported by the present data. Allowing for random errors in the measurements, etc., we estimate a pellet to pellet variability of 5 percent or so; the data for crystals grown with "master alloy" doping, Table 2, has less scatter, but the sample size is too small to draw any statistically valid conclusions. The other data groups represent reasonable sample sizes; by evaluating the grand mean of this data, we calculate $k_{eff} = 0.70 \pm .03$ for boron in dendritic web silicon. Although larger than our previous estimate, this value is still significantly smaller than the generally accepted value of $k_o = 0.8$ obtained during Czochralski growth.

As discussed in the previous annual report[1] a knowledge of the segregation coefficient of boron has both technological and scientific import. From a technological viewpoint, the segregation coefficient is a necessary parameter for determining the addition rate of boron dopant during melt replenishment. From a scientific viewpoint, any variation of solute segregation from the anticipated behavior can provide insight into the basic crystal growth mechanism. In particular, an effective segregation coefficient which is smaller than the "equilibrium" value implies some kinetic effect at the crystal-liquid interface. Such effects have been reported for some solutes in silicon melts under the category of a "facet effect".[3] In such cases the segregation coefficient for a solute impurity differs depending on whether or not the growth front is a (111) facet. Such a faceted growth front, like the one depicted schematically in Figure 8, is entirely plausible. The crystallographic relations for web in fact, permit a faceted growth front made up of (111) planes. Atomic attachment kinetics on the (111) facets would normally inhibit nucleation and growth for such a crystal: however, these constraints are relieved by the reentrant corner where the web joins the bounding dendrite. It is also possible that some layer growth is initiated at the reentrant groove created by the twin planes: however, this must not be an essential mechanism since web crystals have been grown in which the twin planes were present only in the bounding dendrites and not in the web itself.

Dwg. 7696A58

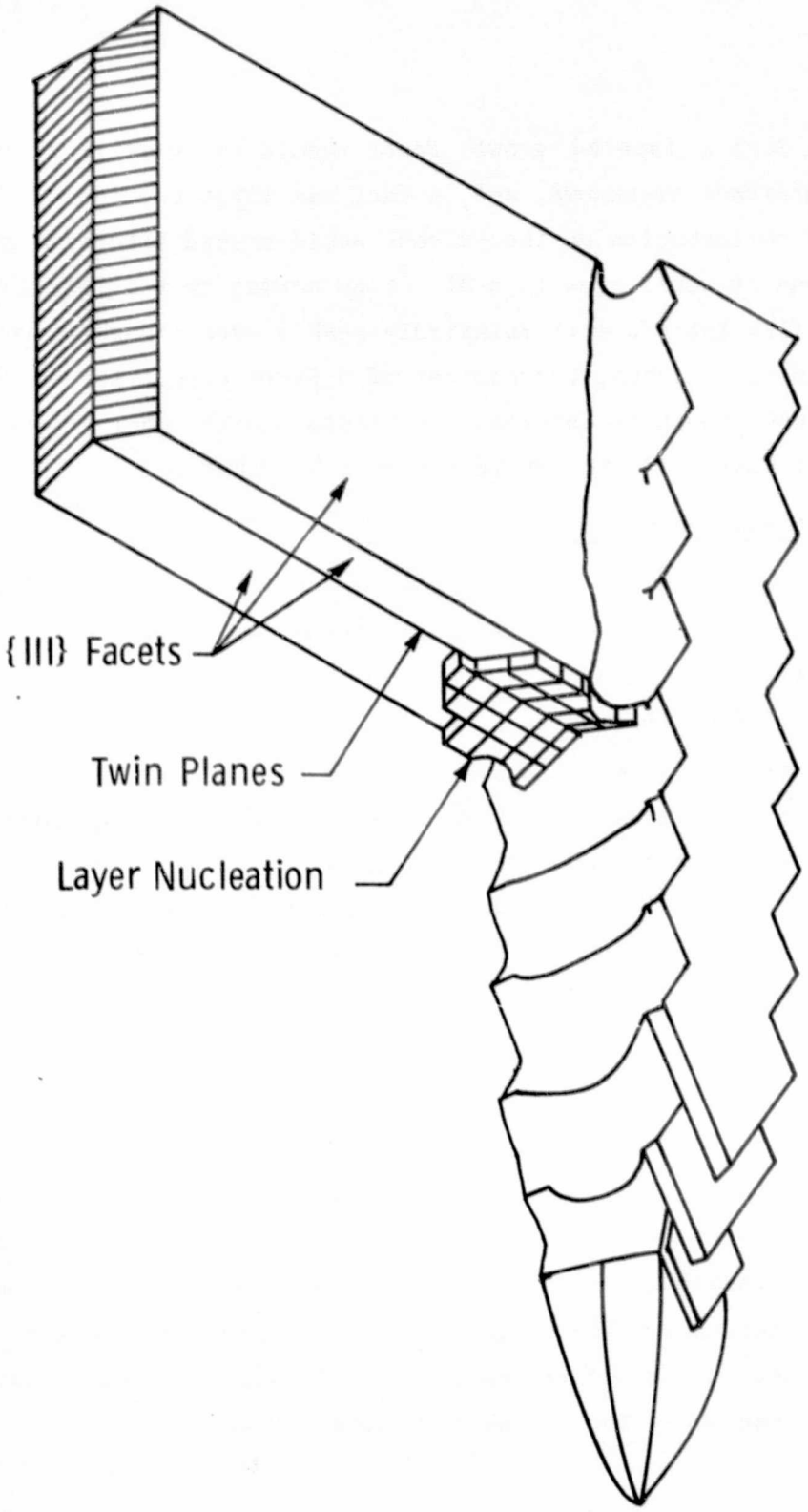

Figure 8 Illustration of a Dendritic Web Growth Interface

Such a faceted growth front should be relatively stable against interface breakdown, and, in fact, was first considered for this reason. A perturbation on the surface would spread laterally much more rapidly than it would grow in a direction normal to the interface, and hence the flat interface is relatively stable even though it grows in a supercooled melt. Thus, the concept of a facet effect for boron in dendritic web growth is internally consistant with other growth behaviour, although it must still be considered as a hypothesis.

3.6 Solar Cell Evaluation

During the report period 53 crystals grown in the RE- and J-furnaces were evaluated by fabricating 1x1cm test solar cells. As usual,[1] two samples were taken from each crystal and two cells fabricated per sample so that four cells were made per crystal. The averaged data for these cells is given in Appendix 9.2. For continuity in the numerical sequence, some previously reported crystal data is also included in the table; current runs are WQ24 to WQ29. Also, all available data for the standard web material are included; these samples are web material which has previously given high quality ($\eta_{AR} \sim 14\%$) cells and are included to verify the processing results.

The data for the current runs gives an average cell efficiency, $\eta_{AR} = 12.06 \pm 0.66\%$ which is somewhat smaller than the corresponding value of $12.72 \pm 0.58\%$ for the cell data reported previously.[1] The reason for this apparent degradation in performance is not completely clear. No changes have been made in the material handling procedures for crystal growing nor has any change been made in the solar cell fabrication sequence. The crystals do, of course, represent a variety of thermal geometries in the growth system. In addition, facilities reorganization has been occurring in the cell fabrication area.

A variety of analytical procedures recently have been instituted to try and discern the causes of the performance shift. A number of cells and web crystals are being evaluated-DLTS data, dark I-V cell characteristics, etc, to try to separate the material and the fabrication aspects.

4. CONCLUSIONS

Although underway only about a month and a half, Phase III of the Silicon Web Development Program has produced some important results. Improvements in thermal shielding above the susceptor growth lid reduced stress sufficiently that web crystals nearly 4.5cm have been grown, the widest so far achieved.

Melt replenishment technology originally tested on the smaller W-furnace system has been successfully transferred to the RE-furnace, a facility which is compatible with high output rate operation. Utilizing a newly designed gas flow management system and modified thermal shielding we have doubled to two hours the period for simultaneous web growth with melt replenishment. Longer periods were hindered by web deformation and icing at higher feed rates, difficulties not apparently associated with replenishment technology per se.

We have identified and bench tested a laser reflection scheme for sensing the silicon melt level in a web growth system. A conceptual design has been made of a level sensing system to control the melt position during melt replenishment; the components have been ordered

A new web growth furnace built at Westinghouse expense is now operational and will be dedicated to the program. This should considerably improve our productivity in developing advanced output rate technology.

We have measured the segregation coefficient of boron in silicon, a parameter required to assure precise doping (resistivity) control in solar cells made from web. We find $k_{eff} = 0.7$ for boron, a value somewhat lower than the 0.8 value for Czochralski pulling. The faceted nature of the web-liquid interface may explain the difference.

5. PLANS FOR FUTURE WORK

During the next quarter we plan to continue the development of methods to increase web width and speed (speed studies will be carried out in the new web furnace) for improved output rate. Growth lids capable of providing extended growth periods will be applied to the replenishment experiments to further raise the sustainable period for growth with replenishment. The laser liquid level sensing apparatus will be assembled and tested for later coupling with the replenishment system.

6. NEW TECHNOLOGY

No new technology is reportable for the period covered.

7. REFERENCES

1. C. S. Duncan, et al., Annual Report, Silicon Web Process Development, DOE/JPL-954654-79/2 April (1979).

2. C. S. Duncan, et al., Quarterly Report, Silicon Web Process Development, DOE/JPL-954654-79/1.

3. M. G. Mil'vidskii and A. V. Berkova, Fiz. Tver. Tela, 5, 709, (1963) Translated: Sov. Phys.-Solid State 5, 517 (1963).

8. ACKNOWLEDGEMENTS

We would like to thank P. A. Piotrowski, H. C. Foust, E. P. A. Metz, W. B. Stickel, J. M. Polito, A. M. Stewart, J. P. Fello, and C. H. Lynn for their contributions to the web growth studies and P. Rai-Choudhury, R. B. Campbell, E. J. Seman, J. B. McNally, W. Cifone, D. N. Schmidt, and H. F. Abt for the processing and testing of the web solar cells.

9. APPENDICES

9.1 Growth Run Summaries

The dominant activity conducted in the J-furnace was testing of lid and shield modifications to improve web width. Maximum area output rates achieved during a run are noted in the result column of the tables. Melt replenishment studies were the main topic for the experiments conducted in the RE furnace. No attempt to achieve high output rate operation was attempted during these runs.

GROWTH RUN SUMMARY

RUN	NO. OF CRYSTALS	LENGTH (cm)	MAX. WIDTH (mm)	MAX. SPEED (cm/min)	DESCRIPTION/RESULT
J-163	3	355	32.5	6.75	Test effect of adding fourth top shield to beveled slot and top shield arrangement of RE-126. Problems with ice suggest that extra shield makes center to end ΔT too small. Reached thruput of 21.7 cm^2/min.
J-164	3	532	35.1	5.74	Return to 3 top shields, beveled lid. Attempt to grow wide web. Improved growth behavior. Max. thruput 20.0 cm^2/min.
J-165	1	305	40.5	1.7	Repeat J-164 configuration. Problems with oxide falling into melt from lid.
J-166	2	180	24.0	1.7	Repeat J-164 Configuration. Difficult to initiate growth. Pull outs. Jumpy melt.
J-167	3	223	24.2	7.5	Repeat J-164 Configuration. Vary growth speed. 18.1 cm^2/min thruput.
J-168	3	292	30.0	5.0	Repeat J-164 configuration. Floating ice problems all day.
J-169	Not Productive of Web				Repeat J-164 configuration. Constant ice problems. Believe this due to oxide particle which fell from lid and attached to crucible wall. Ice spikes from crucible wall.
J-170	1	82	19.1	1.6	Repeat J-164 configuration in attempt to determine cause of erratic behavior. Difficult to get thermal symmetry even with coil adjustment at extreme position.
J-171	3	220	21.2	1.6	Modify top shielding by replacing upper 1.5mm thick shield with one 0.5mm thick in attempt to reduce coupling and run top shield cooler. Consistent ice from left. Coil adjustment (lateral) severely binding to the extent that its function is compromised.

GROWTH RUN SUMMARY

RUN	NO. OF CRYSTALS	LENGTH (cm)	MAX. WIDTH (mm)	MAX. SPEED (cm/min)	DESCRIPTION/RESULT
J-172	2	145	21.6	1.9	Repeat J-171 configuration. Poor growth behavior. After run, coil positioning mechanism overhauled so that it moves freely. However, due to some alignment problems which have apparently increased over a period of time, the range of motion is limited. This will be corrected when time permits.
J-173	3	454	32.8	6.7	Repeat J-171 configuration. Better growth behavior than previous runs, but crystal deformation occurs at narrower widths than in configuration with thick upper top shield. Reached thruput rates of 17.1 and 22.0 cm^2/min.
J-174	2	122	22.2	1.7	Return to J-164 configuration, i.e. 1.5mm Top shield instead of 0.5mm. Difficult to start. Tendency to go poly early.
J-175	3	132	20.1	1.7	Repeat J-174, with similar results. Present inconsistency of behavior of this configuration is not well understood. Perhaps the well used shields have changed sufficiently to perturb thermal behavior. Changes will be made in future runs.

GROWTH RUN SUMMARY

RUN	NO. OF CRYSTALS	LENGTH (cm)	MAX. WIDTH (mm)	MAX. SPEED (cm/min)	DESCRIPTION/RESULT
J-176	2	233	34.2	1.7	Test configuration modification. Overlap of formed lower shield of J-175 configuration increase 1mm. Late start due to servicing of generator. Web deformed at narrower widths than J-175 configuration.
J-177	2	117	20.3	1.7	J-175 configuration. Floating ice in P.M. Dendrites very smooth. Dendrite probe indicated good melt profile.
J-178	No Significant crystal production				J-175 configuration modified by raising upper top shield 1.5mm. Difficult to grow. Web; quality rapidly degenerated.
J-179	No useful crystal production.				Repeat J-178 configuration. Web crystals consistently turned polycrystalline, initiated by formation of a line and subsequent breakdown. Conclude this modification has negative results.
J-180	2	403	40.1	3.5	J-175 configuration modified to uniform 1.5mm shield spacing No argon flow tubes. Good growth, but oxide collected on lower shield.
J-181	3	549	42.1	5.0	J-175 configuration without argon flow tubes. Run terminated due to exhaustion of silicon melt.
J-182	2	434	44.3	1.7	J-181 configuration modified by adding a 0.5mm thick shield on top. New with record, 4.43cm.

GROWTH RUN SUMMARY

RUN	NO. OF CRYSTALS	LENGTH (cm)	MAX. WIDTH (mm)	DESCRIPTION/RESULT
RE-138	5	460	31.4	This was the first run made with aspirators in an elongated susceptor system. The first 40 cm of web pulled had almost no oxide coating, but after another 40 cm the oxide coating was about normal. After the run the aspirators were blocked with oxide. Used RE-1 lid with feed and aspirator holes.
RE-139	4	433	25.5	Repeat of RE-138 set up, but with a decreased aspirator argon flow. The aspirators became blocked with oxide sooner than in RE-138.
RE-140	1	94	21.3	The aspirators were set up to pull gases from between the lid and the shields. The aspirators did not become blocked, but they did not reduce oxide build-up either.
RE-141	4	579	30.7	The purpose of this run was to determine what effect an additional shield in the RE-1 arrangement would have. Growth was easy, but "ice" from oxide spalling and entering the melt ended each crystal, preventing determination of maximum width possible.
RE-142	3	298	26.2	This was the first run made with the milled channel aspirator. The corner with the feed hole and aspirator was too cold; ice from the corner ended several crystals. The lid used had an RE-1 slot.
RE-143	1	216	30.2	Repeat RE-142, with a partial shield on the left end of the susceptor. This solved the problem of freezing in the corner, but some floating ice occurred. A temperature profile of the melt end of the susceptor showed that the feed corner was still too cold.
RE-144	1	169	29.9	Set up as in RE-142, with manual feeder. Several small crystals were started; ice caused pull outs whenever feeding was tried. On the last crystal feeding achieved for 15 minutes before ice appeared.

GROWTH RUN SUMMARY

RUN	NO. OF CRYSTALS	LENGTH (cm)	MAX. WIDTH (mm)	DESCRIPTION/RESULT
RE-145	2	163	20.9	The RE-1 lid with the milled aspirator was used. A partial shield on the right end and a full shield on the left end were used to make the ends of the crucible hotter. The dendrites were choppy and growth was difficult. Twenty five minutes of continuous feeding was performed.
RE-146	2	212	21.4	Set up as in RE-145; Thermal measurements made both with and without feeding. Feeding appeared to drop the temperature on the feed end about 1°. Fed pellets at 1 per minute for 53 minutes before ice appeared.
RE-147	3	473	32.4	Set up as in RE-145, but no argon flow through the feed tube. Heating coil position varied. For one crystal, 83 minutes of feeding at 1 pellet per minute was done before oxide on the lid caused pull out. For the second 85 minutes at 2/min and 33 minutes at 3/min was done before ice appeared. On the third crystal 4 pellets/min were added for 40 min before any ice occurred.
RE-148	3	437	31.1	Set up as in RE-147. For one crystal pellets were added at 3/min for 105 minutes. The crystal was ended because of deformation (problem not caused by feeding).
RE-149	Nonproductive			Set up as in RE-147. Crystals tended to form thirds or pull out easily.
RE-150	2	272	26.3	A growth run, using lid which gave 4cm web. Ice was a major problem; clean-up revealed that there had been a large amount of oxide spalling.
RE-151	6	635	43.1	Set up like RE-150. The first crystals went poly, but after that the crystals grew well.
RE-152	Nonproductive			Run with a lid similar to the RE-1 lid, but with a 1/2" shorter slot. The purpose of running with a shorter slot is to develop more uniform width for feeding experiments.
RE-153	2	268	27.9	Set up like RE-147, but with a lower feed tube position. Oxide collection on the end of the feed tube and in the feed hole prevented successful pellet feeding.

GROWTH RUN SUMMARY

RUN	NO. OF CRYSTALS	LENGTH (cm)	MAX. WIDTH (mm)	DESCRIPTION/RESULT
RE-154	3	338	24.5	First run in development of width control in elongated susceptor. Used J-98A lid and shield arrangement. Growth was difficult; the thermal gradient was quite steep.
RE-155	2	370	29.2	Development of width control; J-98B lid and shield arrangement. Crystals grew well and were easily controlled. Width was stabilizing when the crystal pulled out.
RE-156	1	256	39.1	Lid for wide crystal growth with melt replenishment. No feeding was done; the run checked the ease of growth without replenishment. Web growth was typical; however oxide collected on the bottom shield and brushed against the crystal.
RE-157	3	288	30.9	Repeat of RE-156 lid configuration. Again there was a large amount of oxide on the shield, but during this run oxide fell into the melt ending the crystals.
RE-158	Nonproductive			Used J98-B lid arrangement to try to further develop width control. Ice prevented crystal growth; spalling was the probable cause.
RE-159	Nonproductive			Run aborted when furnace oxidized.
RE-160	Nonproductive			Used J98-B lid arrangement; ice was a problem whether feeding was used or not. Some spalling was evident.
RE-161	2	346	26.7	Used J98-B lid arrangement for width control. There was some ice, but not as much as previously.
RE-162	1	103	19.8	Used same lid as in RE-156, but used a higher aspirator flow; again there was a large amount of oxide growth on the shield. Oxide fell into the melt, ending several crystals rapidly.

GROWTH RUN SUMMARY

RUN	NO. OF CRYSTALS	LENGTH (cm)	MAX. WIDTH (mm)	DESCRIPTION/RESULT
RE-163	Nonproductive			Used same lid as in RE-156, raised the shields by 1/16 inch. This kept the bottom shield clean. Several crystals were polycrystalline; when feeding was tried with several other crystals ice occurred ending growth.
RE-164	3	18.9	31.6	Used same lid as in RE-156; raised shield as in RE-163. A molybdenum block was placed over one dogbone hole in the lid to determine whether this could be used for width control. The block did not collect oxide, and did force crystal to steady state width. Feeding was tried, but resulted in ice.

APPENDIX 9.2

AVERAGED SOLAR CELL DATA FOR WEB CRYSTALS

The tables in this appendix give the averaged solar cell performance for cells fabricated from the crystals listed. Each entry in the table represents the average value for approximately four cells. Measurement conditions were a simulation of an AM1 illumination at a power density of 91.6 mW/cm^2 as determined by a standardized solar cell. The cells were nominally 10x10 mm square (actual area 1.032 cm^2), and had an active area of about 92.5%. The cell efficiency with an anti-reflective coating η_{AR}, is an estimated value based on an average improvement factor of 1.43, typical of the results we obtain in practice with a TiO_2-SiO_2 coating.

RE CRYSTALS

Crystal	Run	I_{sc} mA	V_{OC} Volt	FF	η_o %	η_{AR} %	τ_{OCD} µs	ρ Ω-cm	NOTES
RE-12-3.1	WQ6	22.7	.563	.749	10.1	14.4	41	16.5	Std. Web
	WQ20	22.2	.548	.737	9.5	13.6	11.4		"
	WQ21	22.9	.535	.730	9.5	13.6	13.8		"
	WQ22	21.9	.547	.749	9.5	3.6	22.1		"
	WQ23	22.0	.530	.743	9.1	13.0	18.3		"
	WQ24	22.6	.522	.729	9.1	13.0	8.1		"
	WQ25	21.2	.518	.719	8.5	12.2	8.0		"
	WQ26	22.3	.536	.753	9.5	13.6	20.6		"
RE54-1.2	WQ10	22.3	.555	.735	9.6	13.7	22.6	19.7	Std. Web
	WQ13	23.0	.550	.740	9.9	14.2	19.5		"
	WQ25	21.1	.518	.719	8.3	11.9	9.0		"
	WQ27	21.1	.546	.723	8.8	12.6	19.0		"
	WQ28	21.9	.543	.741	9.3	13.3	18.4		"
	WQ29	21.4	.520	.727	8.6	12.3	7.4		"
RE108-1	WQ22	21.1	.546	.752	9.1	13.0	10.5	16.3	
RE108-2	WQ21	20.2	.516	.738	8.1	11.6	1.1	10.1	
RE108-3	WQ22	19.7	.526	.734	8.1	11.6	2.4	9.9	
RE110-1.2	WQ22	21.3	.543	.748	9.1	13.0	12.0	7.9	
RE110-2.3	WQ22	21.5	.549	.745	9.3	13.3	11.9	8.4	
RE113-2.6	WQ21	19.0	.516	.733	7.6	10.9	1.5	7.4	
RE116-6.3	WQ27	19.3	.528	.736	7.9	11.3	1.7	7.5	
RE120-1.3	WQ24	21.8	.530	.756	9.2	13.2	3.0	7.6	
RE122-1	WQ22	20.5	.544	.742	8.8	12.6	6.8	9.5	
RE123-1	WQ23	20.6	.521	.735	8.3	11.9	3.5		
RE123-5.5	WQ29	20.7	.528	.732	8.5	12.2	4.1	9.5	
-5.11	WQ23	20.1	.511	.733	7.8	11.2	2.2	9.5	Wide
RE124-2.5	WQ24	21.5	.527	.728	8.7	12.4	3.0	8.7	
RE126-2.2	WQ24	20.8	.518	.740	8.5	12.2	1.8	9.8	
RE126-3.3	WQ24	19.9	.512	.701	7.6	10.9	1.4	6.5	
RE126-4.1	WQ24	20.4	.515	.725	8.1	11.6	1.6	6.6	
RE127-1.4	WQ24	21.6	.533	.733	8.9	12.7	3.8	7.4	
RE128-1.2	WQ26	20.8	.533	.752	8.8	12.6	5.7	7.3	

RE CRYSTALS (Cont.)

Crystal	Run	I_{sc} mA	V_{OC} Volt	FF	η_o %	η_{AR} %	τ_{OCD} μs	ρ Ω-cm	NOTES
RE129-2.3	WQ27	20.8	.533	.738	8.6	12.3	5.7	12.6	
RE130-1.4	WQ26	19.6	.522	.743	8.0	11.4	1.8	6.3	
RE130-2.3	WQ26	19.9	.522	.739	8.1	11.6	1.5	5.9	
RE131-2.3	WQ26	21.1	.527	.752	8.8	12.6	4.0		
RE131-3.4	WQ26	20.7	.520	.753	8.6	12.3	2.3	11.9	
RE131-4.3	WQ26	19.3	.500	.724	7.4	10.6	0.8	10.6	
RE132-1.4	WQ26	20.5	.523	.739	8.4	12.0	3.9	10.5	
RE132-2.5	WQ29	20.5	.518	.728	8.5	2.2	4.1	10.6	
RE133-2.4	WQ25	20.2	.522	.728	8.1	11.6	3.2	8.6	
-2.11	WQ25	18.3	.502	.718	7.0	10.0	.8	8.6	Wide
RE134-1.3	WQ27	20.5	.535	.746	8.6	12.3	3.9	8.1	
RE134-2.4	WQ29	20.5	.520	.721	8.1	11.6	3.0	7.7	
RE135-2.4	WQ27	19.7	.527	.732	8.0	11.4	1.8	9.7	
RE136-2.4	WQ27	20.8	.549	.752	9.1	13.0	6.7	7.8	
RE137-2.4	WQ27	19.6	.513	.733	7.9	11.3	2.5	8.3	
RE137-3.1	WQ27	19.9	.505	.724	7.7	11.0	1.5	8.4	
RE138-1.3	WQ27	22.3	.537	.760	9.6	13.7	10.4	7.5	
RE141-1.4	WQ27	21.2	.546	.752	9.2	13.2	9.8	8.1	
RE141-4.4	WQ27	19.2	.516	.725	7.6	10.9	1.4	7.1	
RE143-1.5	WQ27	20.7	.544	.736	8.8	12.6	7.5	8.6	
RE144-1.3	WQ27	20.9	.546	.761	9.2	13.2	10.2	6.4	
RE151-64	WQ29	20.7	.536	.744	8.7	12.4	5.6	8.2	

J CRYSTALS

Crystal	Run	I_{sc} mA	V_{OC} Volt	FF	η_o %	η_{AR} %	τ_{OCD} μs	ρ Ω-cm	NOTES
J10-3.3	WQ29	19.6	.511	.719	7.6	10.9	1.6		
J133-1.6	WQ28	19.2	.510	.724	7.5	10.7	1.2	7.4	
-2.4	WQ20	19.0	.513	.726	7.8	11.2	2.5	10.6	
J134-2.2	WQ20	21.7	.536	.749	9.2	13.2	6.7	10.7	
J134-3.5	WQ28	17.8	.516	.733	7.1	10.2	1.4	7.6	
J135-3.4	WQ29	20.9	.528	.753	8.8	12.6	4.0	7.5	
J140-3.2	WQ21	21.9	.538	.741	9.3	13.3	6.1	6.9	
J154-1.3	WQ24	21.4	.525	.744	8.8	12.6	3.4	8.6	
J164-1.3	WQ28	20.3	.527	.764	8.6	12.3	2.5	9.5	
J164-2.4	WQ29	19.7	.524	.744	8.1	11.6	2.7	8.8	
J168-3.3	WQ29	20.8	.533	.778	9.1	13.0	5.5	7.2	
J173-3.4	WQ29	20.3	.522	.740	8.3	11.9	3.0	10.3	

9.3.1

MILESTONE CHART

JPL CONTRACT 954654

PHASE III

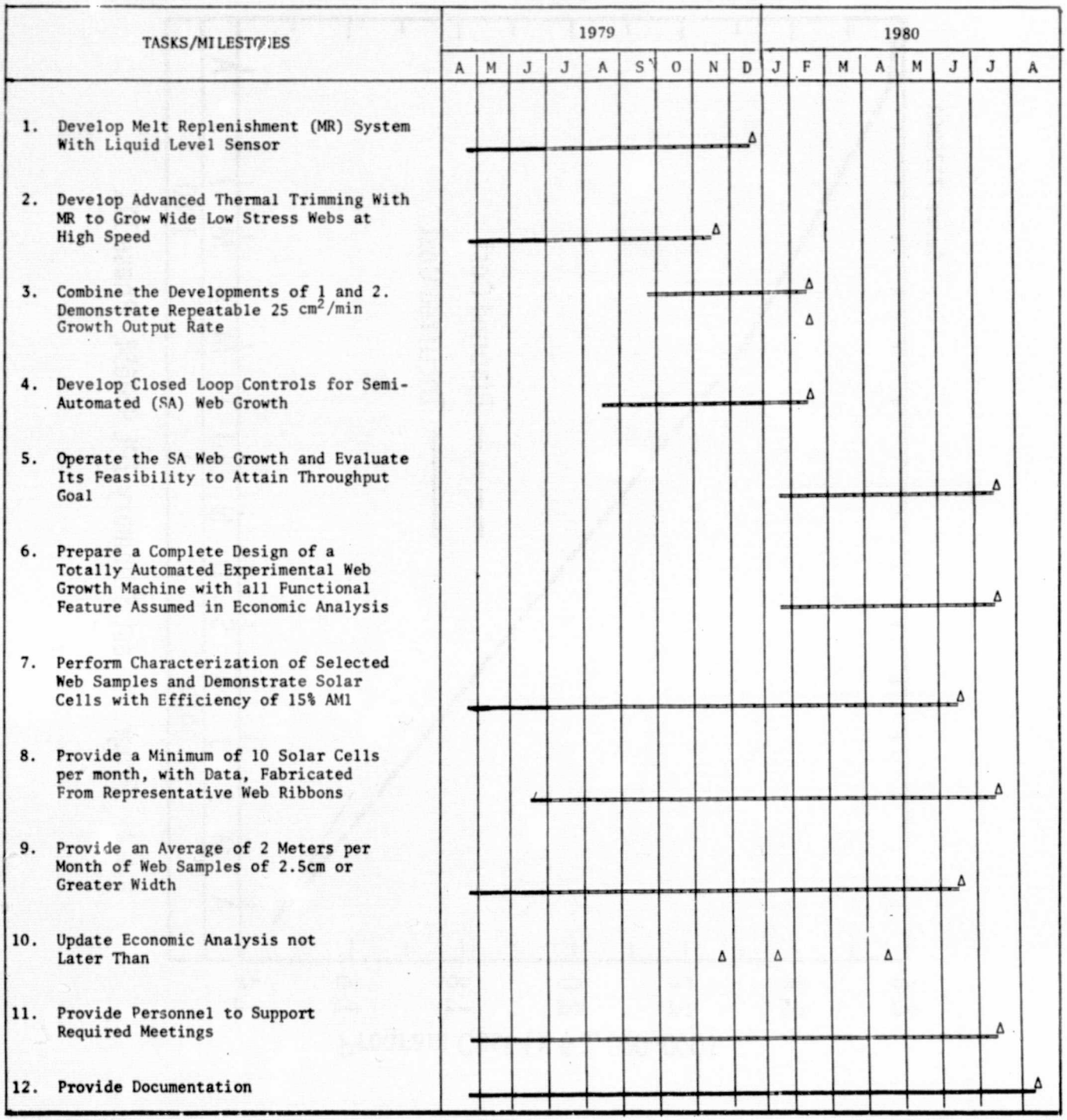

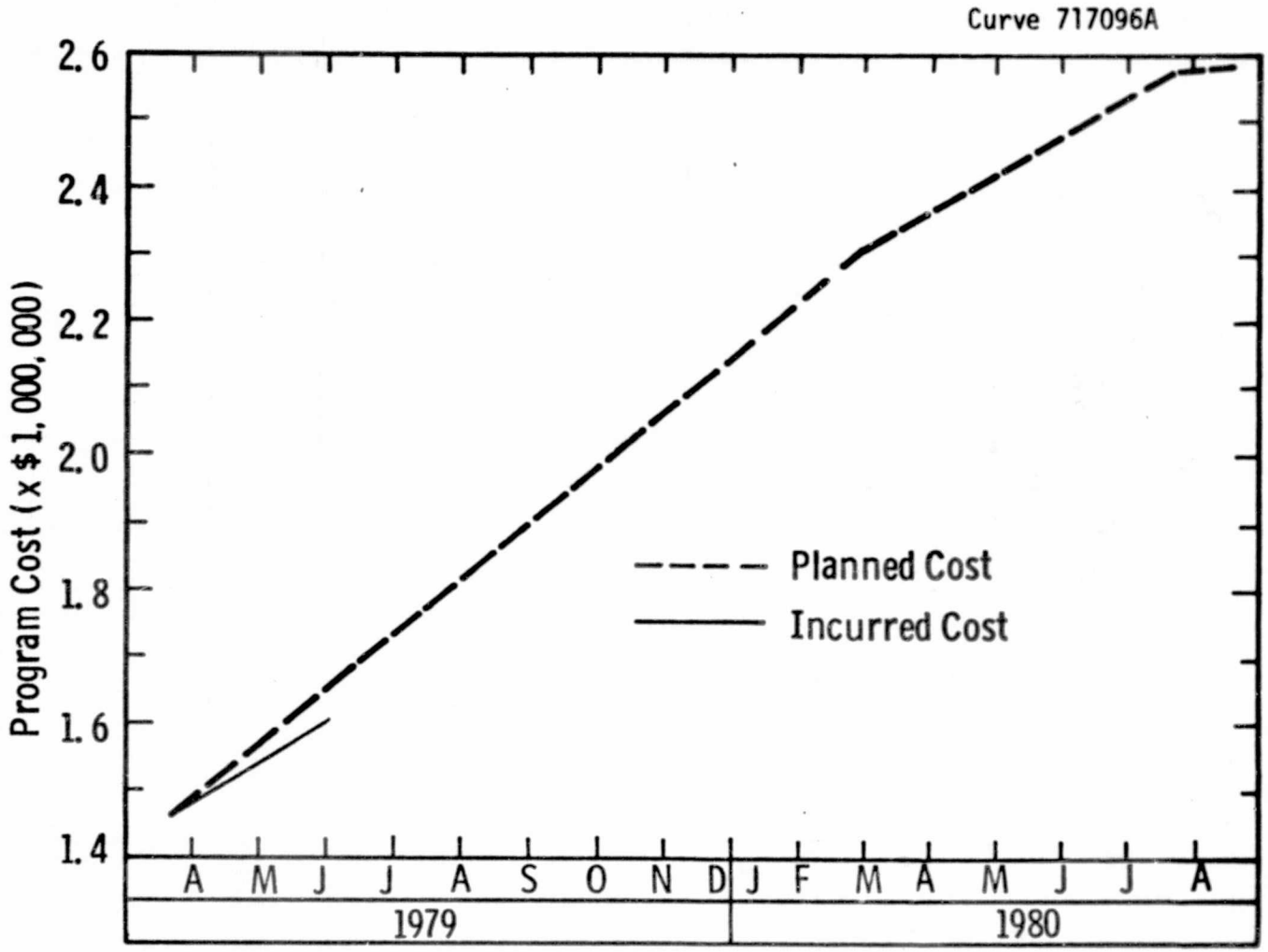

9.3.2 Program Cost Summary JPL 954654, Phase III

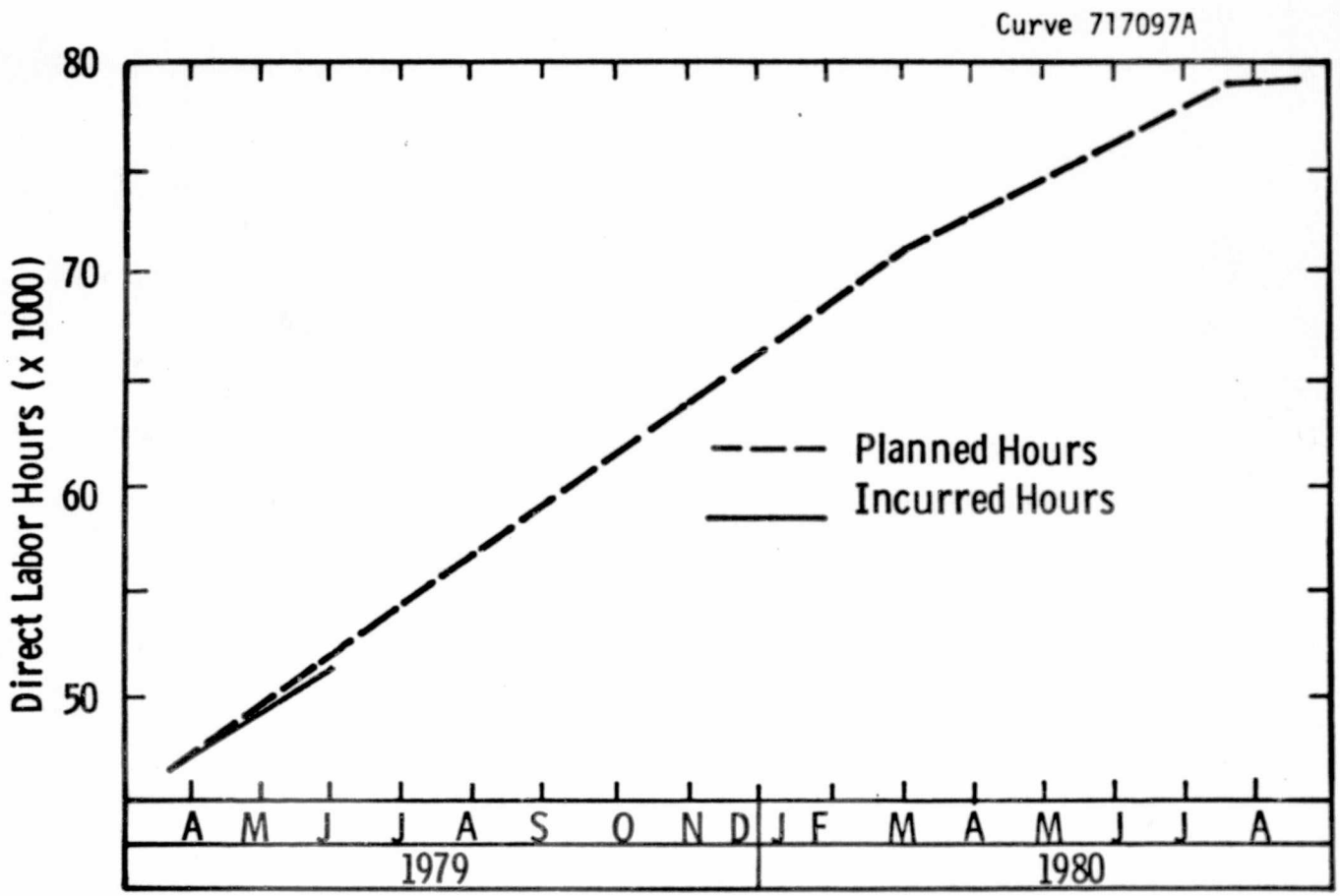

9.3.3 Program Labor Summary JPL 954654, Phase III